

Basolateral Membrane Potential of a Tight Epithelium: Ionic Diffusion and Electrogenic Pumps

S.A. Lewis*, N.K. Wills*, and D.C. Eaton

Department of Physiology and Biophysics, University of Texas Medical Branch,
Galveston, Texas 77550

Received 19 September 1977; revised 23 December 1977

Summary. The contribution of specific ions to the conductance and potential of the basolateral membrane of the rabbit urinary bladder has been studied with both conventional and ion-specific microelectrode techniques. In addition, the possibility of an electrogenic active transport process located at the basolateral membrane was studied using the polyene antibiotic nystatin. The effect of ion-specific microelectrode impalement damage on intracellular ion activities was examined and a criterion set for acceptance or rejection of intracellular activity measurements. Using this criterion, we found $(K^+) = 72$ mM and $(Cl^-) = 15.8$ mM. Cl^- but not K^+ was in electrochemical equilibrium across the basolateral membrane. The selective permeability of the basolateral membrane was measured using microelectrodes, and the data analyzed using the Goldman, Hodgkin-Katz equation. The sodium to potassium permeability ratio (P_{Na}/P_K) was 0.044, and the chloride to potassium permeability ratio (P_{Cl}/P_K) was 1.17. Since K^+ was not in electrochemical equilibrium, intracellular (K^+) is maintained by active metabolic processes, and the basolateral membrane potential is a diffusion potential with K^+ and Cl^- the most permeable ions. After depolarizing the basolateral membrane with high serosal potassium bathing solutions and eliminating the apical membrane as a rate limiting step for ion movement using the polyene antibiotic nystatin, we found that the addition of equal aliquots of NaCl to both solutions caused the basolateral membrane potential to hyperpolarize by up to 20 mV (cell interior negative). This potential was reduced by 80% within 3 min of the addition of ouabain to the serosal solution. This hyperpolarization most probably represents a ouabain sensitive active transport process sensitive to intracellular Na^+ . An equivalent electrical circuit for Na^+ transport across rabbit urinary bladder is derived, tested, and compared to previous results. This circuit is also used to predict the effects that microelectrode impalement damage will have on individual membrane potentials as well as time-dependent phenomena; e.g., effect of amiloride on apical and basolateral membrane potentials.

Many of the so-called tight epithelia transport Na^+ from the lumen to the blood. The original model for Na^+ transport across tight epithelia, as devised by Koefoed-Johnsen and Ussing (1958), visualized Na^+ pas-

* *Present Address:* Department of Physiology, Yale Medical School, 333 Cedar Street, New Haven, Connecticut 06510.

sively entering the cell from the lumen across the apical membrane, thus the apical membrane acted as a Na^+ electrode. After entering the cell, it was postulated that Na^+ was actively pumped across the basolateral (blood side) membrane in a 1:1 exchange for K^+ . Consequently, the basolateral membrane was thought to act as a K^+ electrode.

Recent research has indicated that the apical membranes of some tight epithelia [rabbit urinary bladder (Lewis *et al.*, 1977); and rabbit descending colon (Schultz, Frizzell & Nellans, 1977; Turnheim, Frizzell & Schultz, 1977)] do act as Na^+ electrodes in agreement with the model, although there is a conflict concerning the source of the apical membrane potential in frog skin (Fuch, Hviid Larsen & Lindemann, 1977; Helman & Fisher, 1977) and toad urinary bladder (Finn, 1976; Sudose & Hoshi, 1977). Moreover, some evidence indicates that the properties of the basolateral membrane, as described by Koefoed-Johnsen and Ussing (1958) might not be correct (Finn, 1976). Thus, the basolateral membrane might be permeable to other ions, e.g., Na^+ and Cl , and the $\text{Na}^+ - \text{K}^+$ transport system might not be electrically silent but might have a coupling ratio different from unity.

The present paper is aimed at investigating the passive permeability and the active Na^+ transport of the basolateral membrane of the rabbit urinary bladder using conventional and ion-specific electrodes as well as the antibiotic nystatin.

We have chosen the rabbit urinary bladder as our experimental tissue because of the large cell size, homogeneous cell population in the most apical cell layer, and almost infinite junctional resistance. The transport properties of the rabbit urinary bladder have been previously described in detail (Lewis & Diamond, 1975, 1976; Lewis, Eaton & Diamond, 1976; Lewis, 1977*a*; Lewis *et al.*, 1977).

Materials and Methods

Urinary bladders were obtained from adult New Zealand white rabbits. The tissue was dissected, mounted according to the procedures of Lewis and Diamond (1976), and placed between modified Ussing chambers (15 ml/chamber) which were designed to eliminate edge damage and to reduce hydrostatic gradients during microelectrode impalements (*see* Lewis, 1977*a-b*; Lewis *et al.*, 1977).

Electrical Measurements

Transepithelial voltage (V_t) was monitored with two 100 mm LiCl agar bridges placed 10 mm apart on opposite sides of the tissue and referenced to the serosal solution. Ag

—AgCl electrodes placed at the end of each chamber were used to determine short-circuit current (I_{sc}) and transepithelial capacitance (C_t) (see Lewis and Diamond, 1976). All electrodes led to an automatic voltage clamp. V_t and I_{sc} were displayed on two digital voltmeters (Analogic) and one channel of a multichannel chart recorder (Brush). In addition, these signals, along with microelectrode readings, were interfaced on-line with a PDP-8/E laboratory computer (Digital). All voltages were measured within ± 0.1 mV.

Microelectrodes

Conventional microelectrodes were constructed from fiber-filled Pyrex tubing (OD = 1 mm) which was pulled on a horizontal pipette puller (Industrial Associates). Microelectrodes were filled with 3 M KCl and had tip resistances of 20–80 M Ω . Microelectrodes were connected to a differential electrometer (WP Instruments, Model 740) referenced to the serosal solution. Fine positioning of the microelectrode was achieved within ± 1 μ m with a hydraulic microdrive (Stoelting).

K⁺ Sensitive Microelectrodes

Single-Barreled. Single barreled microelectrodes were constructed according to methods described by Walker (1971) and Eaton, Russell and Brown (1975). Briefly, Pyrex® capillary tubing was pulled to a tip of less than 1 μ m diameter (mean resistance ≈ 20 m Ω when filled with 3 M KCl). Microelectrode tips were dipped in a 2.5% solution of trichloro-n-butyl silane in α -chloronaphthalene for about 15 sec and then baked at 250 °C for 30 min. Afterwards, the tips were back-filled to a distance of approximately 250 μ m from the tip with K exchanger (Corning Glass Works). The remaining portion of the electrode was filled with 0.5 M KCl. The microelectrode was then allowed to equilibrate in NaCl Ringer's (see *Solutions*) for approximately 10 min. For calibration, the response of the microelectrode was tested in 10^0 , 10^{-1} and 10^{-2} M KCl solution. Usable electrodes demonstrated a 58–60 mV change per decade change in potassium activity with a response time less than 1 sec. The selectivity ratio of K⁺ to Na⁺ was estimated to be greater than 50:1.

Double-Barreled. Double barreled microelectrodes were fabricated from two lengths of Pyrex tubing which were pulled together in a Kopf vertical micropipette puller. The tip of the microelectrode was dipped in a solution of 3% tri-chloro-n-butyl silane in chloronaphthalene until approximately 100 μ m of solution entered the tip. The double-barreled microelectrodes were then baked and filled similarly to the single-barreled microelectrodes. The second barrel was filled with 0.5 M Na₂SO₄.

Cl⁻ Sensitive Microelectrode

The chloride sensitive microelectrode was constructed identically to the single barreled K⁺ sensitive electrode, except that a different silanizing agent and liquid exchanger were employed. Microelectrodes were dipped in a 1.5% solution of siliclad® in chloronaphthalene and baked for 1 hr at 250 °C. Chloride liquid exchanger (Corning Glass Works) was introduced into the tip and the barrel filled with 1 M KCl solution. The microelectrode tip was immersed in NaCl Ringer's overnight, then calibrated in 10^0 , 10^{-1} and 10^{-2} M KCl solutions. Because of difficulty with blockage of the electrodes by

silanizing agent, Cl electrodes have somewhat larger tip diameters than either conventional or K^+ electrodes (mean tip diameter $1.5\ \mu\text{m}$).

Because the impedance of ion-sensitive microelectrodes was relatively high (10^8 – $10^{10}\ \Omega$), potentials were measured with a high input impedance Teledyne Philbrick 1035 operational amplifier ($\approx 10^{13}\ \Omega$). All ion-sensitive microelectrodes were recalibrated after each recording session.

Calculation of Activity

To record intracellular ion activity, ion-sensitive microelectrodes were juxtaposed to the apical membrane and a voltage reading in the mucosal solution noted (V_o). The electrode was advanced across the membrane into the cell cytoplasm. Intracellular ion activity (a_x^i) was calculated from the following equation (Eaton *et al.*, 1975):

$$a_x^i = a_x^o \left[\exp \frac{nFz}{Rt} (V_i - V_o - V_{bl}) \right] \quad (1)$$

where a_x^i and V_o are defined above, V_{bl} is the basolateral potential, V_i is the ion-sensitive microelectrode reading inside the cell, z the valence of the ion, and n is a correction factor for nonideal slopes (V^{ideal}/V_o). Initially, V_o is arbitrarily set to zero in the mucosal solution. If during the course of the experiment the reading in the mucosal solution does not remain zero, a correction for the drift can be made; however, in our experiments, changes in V_o were always less than 1 mV. Corrections for competing ions were ignored for K^+ since the K^+ sensitive microelectrodes were highly selective for potassium over sodium and similarly ignored for Cl^- as the identity of the competing anions (and their activity coefficients) was unknown.

For single-barreled microelectrodes, estimates of V_{bl} were obtained from conventional microelectrode readings taken in the period 10 min before and after the ion-sensitive microelectrode recording. V_{bl} was estimated as the mean value of equal numbers of conventional microelectrode impalements taken from each period. The activities calculated with this method agreed with the results from double-barreled recordings (*see Results*).

Control for Impalement Damage. Lindemann (1975) has expressed concern that microelectrode impalement of small epithelial cells may introduce significant damage and thus shunt conductance to cell members. In the present study, such damage could lead to leakage of ions into or out of the cytoplasm and, consequently, result in serious underestimation or overestimation of intracellular K^+ and Cl^- activities, respectively. To control for this possibility, the voltage divider ratio ($\alpha \equiv G_{bl}/G_a$) was compared to transepithelial conductance (G_t), when G_t was increased by mucosal addition of the antibiotic, nystatin. In the absence of a significant shunt conductance, the relationship of α to G_t is essentially linear $G_t = G_j + G_{bl}(1 + \alpha)^{-1}$ where G_j is junctional conductance (Lewis *et al.*, 1977). Presence of a microelectrode shunt, on the other hand, causes deviations from linearity at low $(1 + \alpha)^{-1}$ values. Further criteria for the acceptance or rejection of particular impalements will be discussed in the results.

Solutions

The composition in mM of the usual bathing solution (NaCl Ringer's) was 111.2 NaCl, 25 NaHCO_3 , 5.8 KCl, 2.0 CaCl_2 , 1.2 MgSO_4 , 1.2 KH_2PO_4 and 11.1 glucose. This solution was gassed with 95% O_2 –5% CO_2 and maintained at a pH of 7.4 and

Table 1. Composition for constant KCl product bathing solutions (in mM)

Solution	Na ⁺	K ⁺	Cl ⁻	Ca ²⁺	Mg ²⁺	HCO ₃ ⁻	H ₂ PO ₄ ⁻	SO ₄ ⁻²	MeSO ₃ ⁻	Sucrose	Glucose
Na ₂ SO ₄	150	0	0	10	1.2	25	1.2	63.1	20	120	11.1
K ₂ SO ₄	0	150	0	10	1.2	25	1.2	63.1	20	120	11.1
NaCl	169.8	0	150	2	1.2	25	1.2	0	0	0	11.1

Composition of bathing solutions for constant KCl product solutions. #1-3 are stock solutions which were combined in the appropriate proportions to produce the desired experimental solutions.

temperature of 37°C. Usually "NaCl Ringer's" was employed as a standard bathing solution. "KCl Ringer's" or "choline Cl Ringer's" differed from the standard solution by equimolar replacement of NaCl—NaHCO₃ with these salts; all other solutes remained at the same concentration. The composition in mM of the K₂SO₄ Ringer's was 58.5 K₂SO₄, 25 KHCO₃, 10 Ca (methanesulfonate)₂, 1.2 MgSO₄, 1.2 KH₂PO₄, 11.1 glucose, 80 sucrose. Constant KCl product solutions were made by mixing the appropriate volumes of the three solutions listed in Table 1. The constant KCl product solutions were hypertonic to the "NaCl Ringer's" by 40 mosmol. An equal increase in the tonicity of the "NaCl Ringer's" did not alter transport properties.

We observed that use of "K₂SO₄" solution in the mucosal chamber caused no change in the transepithelial resistance but did result in a slow depolarization of the basolateral membrane potential. To explain this result, it is possible that either a liquid junction potential existed between the mucosal K₂SO₄ solution and LiCl agar bridges as compared to the serosal NaCl solution and LiCl agar bridges or that an intrinsic property of the K₂SO₄ salt altered cellular integrity.

We found that for the K₂SO₄ Ringer's there was a negligible junction potential. Therefore, our slow depolarization must be caused by some property of the K₂SO₄ salt. If the K₂SO₄ salt crystals were first ashed at 1000 °F for 12 hr, the change in potential no longer occurred. Possibly some organic contaminant of the K₂SO₄ may have been responsible for the depolarization. Because of this, all K₂SO₄ and Na₂SO₄ salts were routinely ashed.

Activity Coefficient for K₂SO₄

Due to the lack of information concerning the activity coefficient for different K⁺ concentrations in a K₂SO₄ solution, we used a K⁺ selective microelectrode to measure this activity. The K⁺ electrode was calibrated before and after the series of measurements in K₂SO₄ solutions, and also electrode drift was monitored with a standard KCl (100 mM) between each K₂SO₄ solution to guarantee that the sulfate salt was not affecting the exchanger. A flowing bridge calomel electrode was used as solution ground. Figure 1 is a semilogarithmic plot of total K⁺ concentration in the K₂SO₄ solutions against the calculated activity coefficient at 21 °C.

Throughout this paper we will use brackets [] to indicate concentration and parenthesis () to indicate activities.

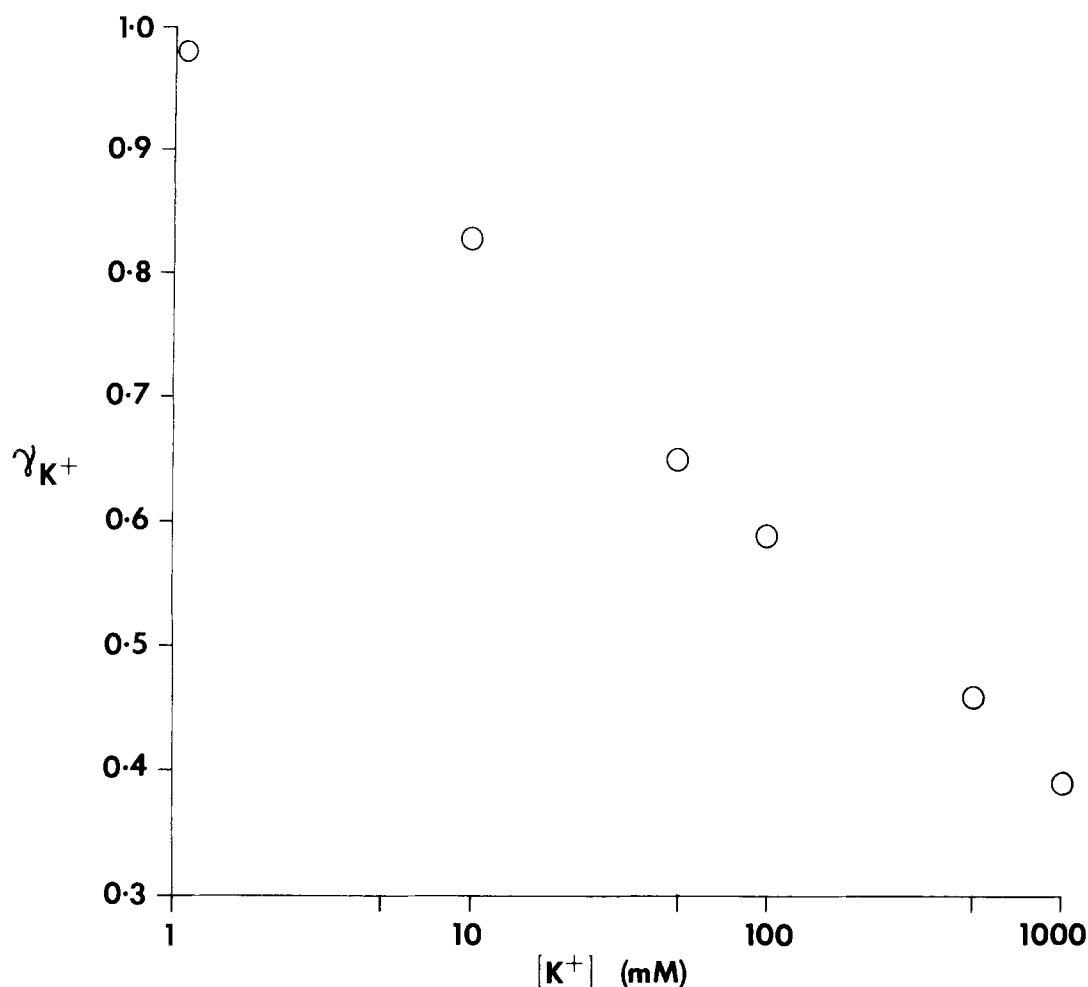


Fig. 1. K⁺ activity coefficient () vs. K concentration (mM) (Sulfate salt) were measured with a liquid K⁺-exchanger microelectrode referred to a flowing bridge calomel electrode

Results

Intracellular K⁺ Activities

Both single barrel (SB) and double barrel (DB) K⁺ selective electrodes were used to measure the intracellular (K⁺) of the most apical cell layer of the rabbit urinary bladder. Figure 2a is a histogram of the intracellular K⁺ activity. This histogram shows a bimodal distribution. Two possible explanations for this distribution are: (i) there are two cell populations, each having distinct intracellular (K⁺) or (ii) because of

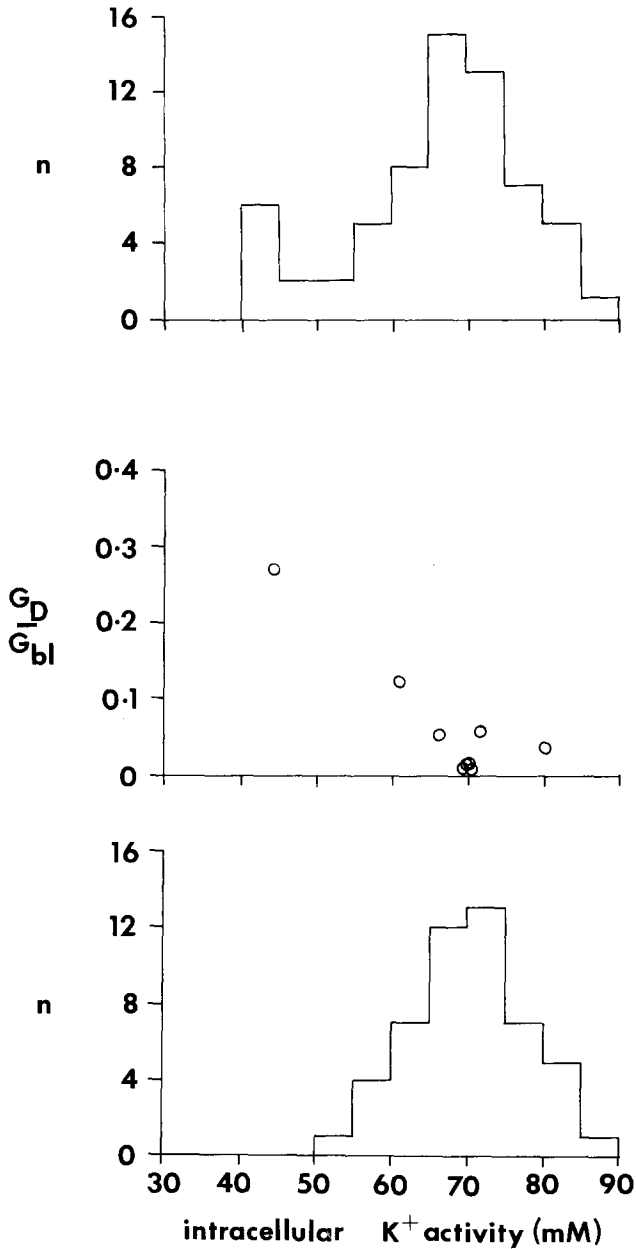


Fig. 2. Summary of K^+ selective microelectrode impalements. *Top panel:* Frequency histogram of K^+ activity measurements (K^+). *NOTE:* the bimodal distribution with the most frequent measurement occurring at 40 and 65 mM. *Middle panel:* K^+ activity as a function of impalement damage conductance (G_D) and basolateral membrane conductance (G_{bl}). *NOTE* that G_D/G_{bl} is greatly increased at lower (K^+) values. *Lower panel:* Corrected frequency histogram using the rejection criteria of $G_D/G_{bl} < 0.1$. *NOTE* that the sample now appears to be normally distributed

normal variation in tip diameters, some of the K^+ sensitive electrodes introduced a significant shunt into the apical membrane of the impaled cell resulting in a loss of intracellular K^+ and decrease in the basolateral potential. The second alternative is possible since there is no good method for assessing random variations in the tip size of the ion-specific electrodes as there is with conventional electrodes in which abnormal tip sizes can be detected by measurements of resistance after filling with 3 M KCl.

Since the most apical cell layer of the rabbit bladder is composed of a homogeneous cell population, the first explanation seems unlikely. The second possibility, of the K^+ electrode introducing a significant leak in the apical membrane, was assessed by comparing the α recorded by a conventional microelectrode (α_c) to that recorded by the SB and DB K^+ electrodes (α_{K^+}). Lewis *et al.* (1977), using the polyene antibiotic nystatin, demonstrated that conventional microelectrodes selected to have tip resistances greater than 20 M Ω did not cause shunt damage in the apical membrane of rabbit bladder during cell impalement. Thus, by comparing the two α measurements we can directly determine the ratio of damage conductance (G_D) in the apical membrane to the conductance of the basolateral membrane (G_{bl}) by the following formulation:

$$(\alpha_{K^+})^{-1} - (\alpha_c)^{-1} = G_D/G_{bl} \quad (2)$$

where

$$\alpha_{K^+} = \frac{G_{bl}}{G_a + G_D} \quad \text{and} \quad \alpha_c = \frac{G_{bl}}{G_a}$$

and G_a is the conductance of the undamaged apical membrane (Lewis *et al.*, 1976; Lewis, 1977a-b).

Figure 2b is such a plot of G_D/G_{bl} on the ordinate and measured intracellular (K^+) on the abscissa. This figure demonstrates that as the ratio of the damage conductance to basolateral conductance increases, intracellular (K^+) decreases. Such an increase in this ratio accounts for the bimodal distribution of the (K^+) in the histogram, since the (K^+) at a conductance ratio of less than 0.1 remained constant (i.e., the damage conductance is less than one tenth the basolateral conductance), while above this ratio the measured activity rapidly decreases. Consequently, we have chosen to reject intracellular (K^+) measurements which have a conductance ratio greater than 0.1. Figure 2c is a histogram of intracellular (K^+) using the described rejection criterion. As can be seen, the histogram appears to show a normal distribution of intracellular (K^+).

Table 2.

	V_{bl}	V_{K^+}	(K ⁺)	α_{K^+}	α_{conv}	V_T	R_T	N	Animals	Slope elec.
(A) DB	-43.3 ± 2.2	17.8 ± 2.9	66.3	10.5 ± 6	15 ± 7	20 ± 1.2	29 ± 3.2	19	2	58
(B) SB	-53.8 ± 6.3	9.6 ± 5	72.0	15.8 ± 13	18 ± 5	35 ± 2.5	29 ± 1.2	31	5	58
(C) SB (Ouabain)	-26 ± 6	4.7 ± 7	32	15 ± 10	15 ± 5	6 ± 1	15 ± 1	11	2	58
		V_{Cl^-}	(Cl ⁻)	α_{Cl^-}						
(D) SB	-52 ± 1	7.4 ± 5	15.8	10	15	32 ± 8.2	28 ± 0.2	10	1	55

Ion sensitive microelectrode impalements: The table contains a summary of various membrane parameters as measured with different methods. The parameters tabulated are basolateral potential (V_{bl}), ion electrode potential (V_{K^+} or V_{Cl^-}), ion activity (K⁺ or Cl⁻), the voltage divider ratio with the ion specific electrodes (α_{K^+} or α_{Cl^-}) and the same ratio obtained with conventional electrodes (α_{conv}), and the transepithelial potential and resistance (V_T and R_T). (A) and (B): K⁺ activity (K⁺) as measured by K⁺ sensitive (liquid ion exchanger) microelectrodes. DB=double barrel and SB=single barrel microelectrodes. All reported impalements met a rejection criterion: $D_G/G_{bl} < 0.1$ (for details see text). (C): Same data after incubation of bladders with 10^{-4} ouabain. Note decreases in V_{bl} and intracellular (K⁺). (D): Intracellular Cl⁻ activity measurements (Cl⁻). Activities in Lines A–D were calculated from Eq. (1) in text. All potentials are in mV, activities in mM, and resistance in k Ω μ F.

Table 2 summarizes the intracellular (K⁺) measured with both DB and SB K⁺ selective microelectrodes using the above rejection criterion. V_{bl} is the spontaneous basolateral potential (cell interior negative with respect to the serosal solution). V_{K^+} is the potential measured between the K⁺ selective electrode and the serosal solution. Equation (1) was used to calculate the intracellular (K⁺). V_o was zero for all experiments.

The top two lines give values for double barrel and single barrel electrodes in normally transporting bladders. The third line is the intracellular (K⁺) after two bladders were incubated with 10^{-4} M ouabain in the serosal solution for one hour; note that both basolateral potential and intracellular (K⁺) have decreased, as has transepithelial resistance (see Lewis & Diamond, 1976).

The fourth line of values is a measurement of the intracellular (Cl⁻) for one bladder. After correction for the slope, the calculated intracellular (Cl⁻) was 15.8 mM. If Cl⁻ was passively distributed at a membrane potential of 52 mV (cell interior negative), the intracellular (Cl⁻) would be 12.9 mM. Our measured value of 15.8 mM is in good agreement with the equilibrium value considering that even a minor amount of impalement shunt would very rapidly increase the intracellular (Cl⁻).

Selective Permeability of the Basolateral Membrane

In NaCl Ringer's the cell interior was always electrically negative to the serosal solution and independent of the rate of Na^+ transport (mean rate of transport of $2 \mu\text{A}/\mu\text{F}$). To determine the selective permeability of the basolateral membrane we measured, using microelectrodes, the change in the basolateral membrane potential under two conditions of altered serosal solution ion composition: constant KCl product to determine $P_{\text{Na}}/P_{\text{K}}$; and constant Cl^- with equimolar replacement of Na^+ for K^+ .

1. *Sodium to potassium permeability ratio.* The $P_{\text{Na}}/P_{\text{K}}$ of the basolateral membrane was determined by measuring the change in the basolateral membrane potential (ΔV_{bl}) when Na^+ was replaced with K^+ (mass balance was maintained) while maintaining a constant KCl product (see Table 1 for composition of constant KCl product solutions).

The potential change (ΔV_{bl}) elicited when the serosal solution was changed from an initial solution with high Na^+ $[(\text{Na}^+)_o^i]$ and low K^+ $[(\text{K}^+)_o^i]$ to a solution with an altered Na^+ $[(\text{Na}^+)_o^x]$ and K^+ $[(\text{K}^+)_o^x]$ can be expressed as:

$$\Delta V_{bl} = \frac{RT}{ZF} \ln \frac{(\text{K}^+)_o^i + P_{\text{Na}}/P_{\text{K}}(\text{Na}^+)_o^i}{(\text{K}^+)_o^x + P_{\text{Na}}/P_{\text{K}}(\text{Na}^+)_o^x} \quad (3)$$

assuming that Cl^- is passively distributed and, consequently, does not alter the membrane potential. No correction for the effect of junctional conductance on the basolateral potential was made because of the extremely low junctional conductance.

The measured membrane potential changes were fit to Eq. (3) as a function of the external (serosal) (K^+) using a nonlinear least squares curve fitting procedure. The initial K^+ activity, $(\text{K}^+)_o^i$ was 1.9 mM. Serosal (K^+) was changed from 1.9 to 15 mM (we used the Guggenheim assumption for correction of activities). Above a value of 15 mM we found irreversible depolarization of the basolateral membrane indicating an increase in the leak conductance for the membrane. The $P_{\text{Na}}/P_{\text{K}}$ derived from the curve fit was 0.044 (Fig. 3).

2. *Chloride to potassium permeability ratio.* The $P_{\text{Cl}}/P_{\text{K}}$ of the basolateral membrane was calculated in a manner similar to that for $P_{\text{Na}}/P_{\text{K}}$ with the exception that external (Cl^-) was maintained at a constant value of 92 mM. The equation used for fitting the data was:

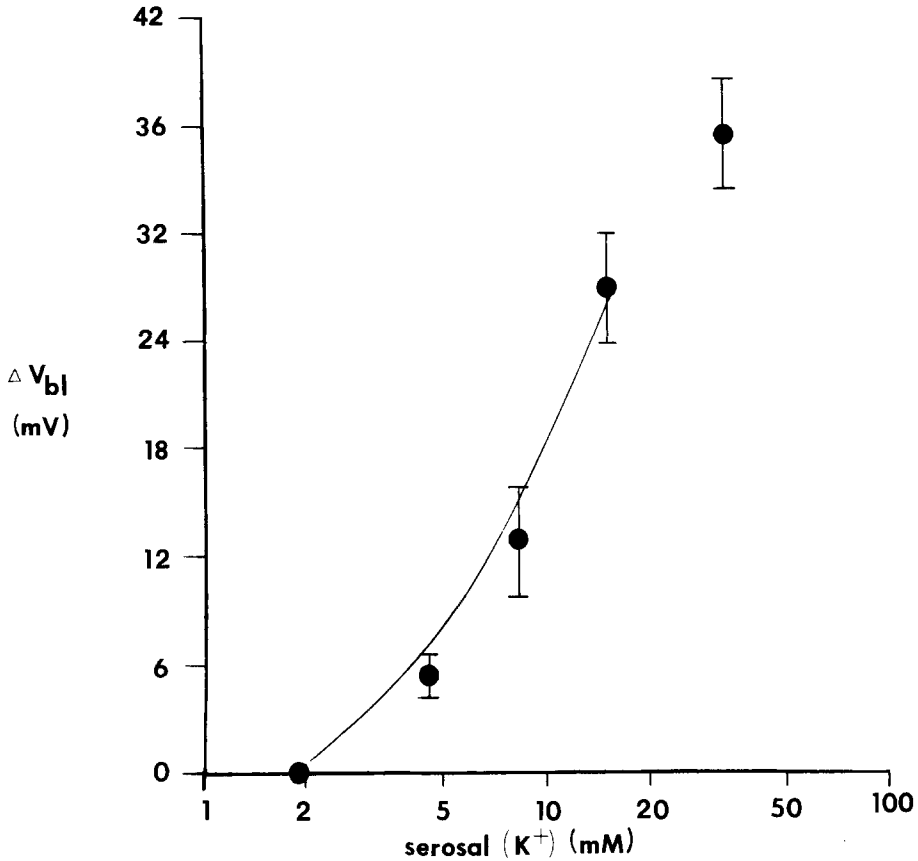


Fig. 3. Changes in V_{bl} as a function of serosal K^+ activity (mM) (constant KCl product). P_{Na}/P_K of 0.044 was estimated from the Goldman-Hodgkin-Katz equation by a least squares nonlinear curve-fitting routine

$$\Delta V_{bl} = \frac{RT}{ZF} \ln \frac{(K^+)_o^i + P_{Na}/P_K (Na^+)_o^i + P_{Cl}/P_K (Cl^-)_i^i}{(K^+)_o^x + P_{Na}/P_K (Na^+)_o^x + P_{Cl}/P_K (Cl^-)_i^x} \quad (4)$$

where $(Cl^-)_i^i$ is the initial intracellular Cl^- concentration and $(Cl^-)_i^x$ is the intracellular Cl^- activity when Na^+ is partially or wholly replaced with K^+ . We assume that $(Cl^-)_i^i = (Cl^-)_i^x$ since the measurements were made immediately after the solution change¹. The value used for $(Cl^-)_i$

1 The change in V_{bl} after increasing serosal (K^+) was *bi*-phasic. First there was a rapid depolarization followed by a slow depolarization. We feel that the rapid depolarization represents the potential change caused by increasing serosal (K^+) . Since Cl^- was found to be passively distributed across the basolateral membrane, the slow depolarization most probably reflects a redistribution of Cl^- . Because of this, ΔV_{bl} was set equal to the change of only the rapid depolarizing phase of the basolateral potential. In addition, each experimental solution was bracketed by a control solution.

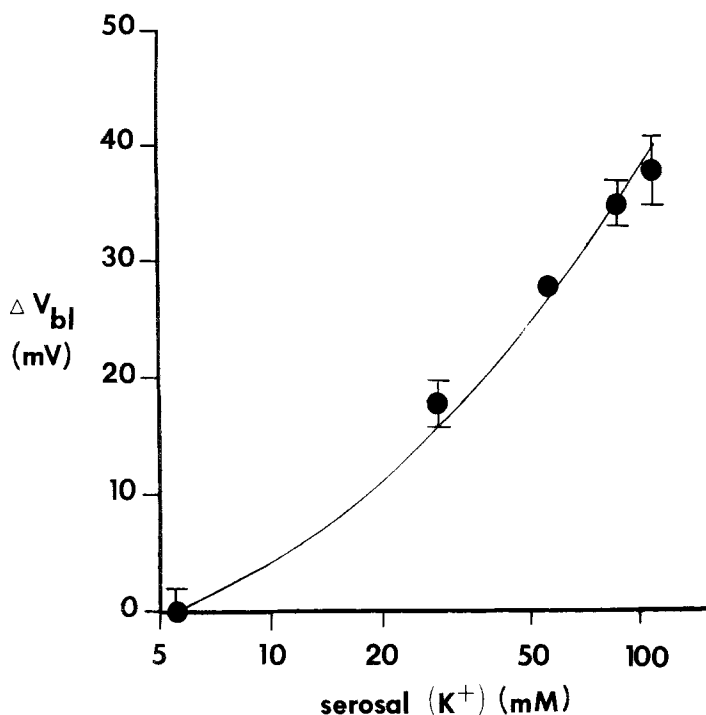


Fig. 4. Changes in V_{bl} as a function of serosal K^+ activity. The Goldman equation was used to fit for P_{Cl}/P_K (ratio = 1.17) while serosal Cl^- was kept constant

was 20 mM (see Table 2) and for P_{Na}/P_K was 0.044. The best fit P_{Cl}/P_K using Eq. (4) was 1.17 (Fig. 4).

Electrogenic Na^+ Transport

In the first section of the results it is obvious that the intracellular (K^+) is not passively distributed across the basolateral membrane, indicating that the intracellular (K^+) is maintained by an active transport system. Cl^- , on the other hand, appears to be passively distributed. The results of the second section suggest that, on the basis of permeability ratios, K^+ is the cation that contributes most significantly to basolateral membrane potential, although changes in Cl^- should also produce large transient changes in membrane potential.

The presence of a diffusion potential does not rule out the possibility of an electrogenic transport system, however. Since Na^+ is the only ion transported across the rabbit bladder, we would expect that Na^+ could be either transported in an electrically silent mode (1:1 coupling of Na^+

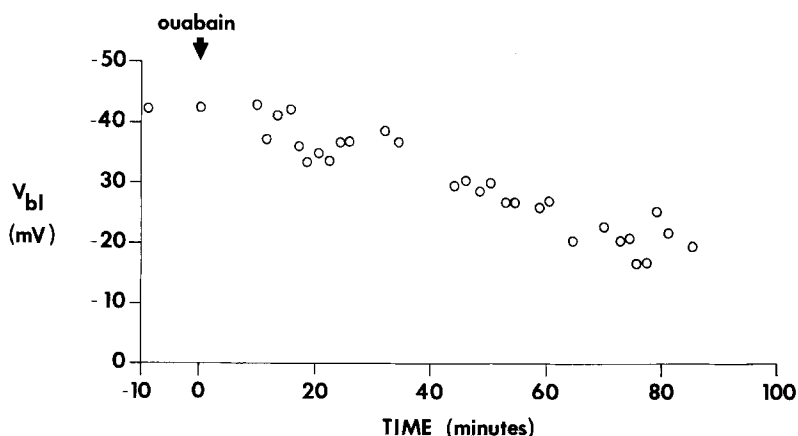


Fig. 5. Effect of ouabain on V_{bl} . Addition of ouabain at time zero is indicated by the arrow. Ouabain induced a 50 % depolarization of V_{bl} within 60–80 min

with K^+ as originally proposed by Koefoed-Johnsen & Ussing, 1958) or in a current producing mode which, because of the direction of current flow (cell to serosal solution), causes a hyperpolarization of the basolateral membrane. We have used two basic approaches to determine the existence of a Na^+ electrogenic pump. The first was to inhibit net Na^+ transport by using mucosal applied amiloride, serosal applied ouabain (10^{-4} M) and mucosal and serosal Na^+ replacement with choline. The second was to increase intracellular $[Na^+]$, using the polyene antibiotic nystatin.

1. Effect of transport inhibitors on V_{bl} . If Na^+ is electrogenically transported across the basolateral membrane, then removal of Na^+ , blockage of Na^+ entry across the apical membrane with amiloride, or inhibition of the suspected electrogenic pump with ouabain should cause a depolarization of the basolateral membrane.

We found that addition of amiloride or replacement of mucosal and serosal Na^+ with choline does not significantly alter the basolateral membrane potential. This finding indicates that if an electrogenic pump is present, the potential it produces is too small to measure.

In excitable tissues the inhibitory action of ouabain on membrane hyperpolarization was found to have a rapid time course (1–3 min for inhibition) (Russell, Eaton & Brodwick, 1977). Thus, if an electrogenic pump is present, we might expect an initial rapid depolarization of the basolateral membrane of rabbit bladder after serosal addition of ouabain. Addition of 10^{-4} M ouabain to the serosal solution of the rabbit

bladder showed no rapid depolarization of the basolateral potential but rather a slow depolarization (Fig. 5), which is consistent with a decrease in intracellular (K^+) (see Table 2).

The bulk of evidence from the above experiments strongly suggests that for normal transport conditions of the rabbit bladder there is no measurable potential associated with the pump in the basolateral membrane. A very probable reason for this negative result is that the rate of net Na^+ transport is too low to cause a significant hyperpolarization of the basolateral membrane. Under normal transporting conditions ($I_{sc} = 2 \mu A$) the basolateral potential would hyperpolarize by at most 2 mV $< (1000 \Omega \text{ basolateral resistance})$.

2. *Alteration of intracellular $[Na^+]$.* The second approach for studying electrogenic Na^+ transport utilizes the polyene antibiotic nystatin to increase apical conductance to Na^+ , thereby raising intracellular $[Na^+]$, resulting in an increased Na^+ supply to the pump.

Lewis *et al.* (1977) found that the addition of the polyene antibiotic nystatin to the mucosal solution of NaCl Ringer's caused the apical membrane resistance to decrease by some 100-fold and caused the basolateral membrane potential to hyperpolarize by some 10 mV, without altering basolateral resistance. Two possible explanations for this hyperpolarization are: (i) the increased intracellular $[Na^+]$ increased the basolateral pumping rate of the $Na^+ - K^+$ ATPase in an electrically silent fashion (1:1 exchange) causing a decrease in (K^+) in the lateral intercellular spaces and an increase in (K^+) in the cell. This will cause a basolateral hyperpolarization by increasing the K^+ gradient from cell interior to serosal solution. (ii) The presence of an electrogenic Na^+ pump that has a $Na^+ - K^+$ coupling ratio greater than 1:1. As we increase the intracellular $[Na^+]$ by increasing the conductance of the apical membrane to Na^+ , the basolateral pump produces an increased net current flow and, thus, hyperpolarizes the membrane.

To separate these two hypotheses, our experimental protocol was as follows: mucosal NaCl Ringer's was replaced with K_2SO_4 Ringer's. 60 μl of nystatin was placed in the mucosal solution, and the change in R_t , V_t and α followed. After the parameters had reached a steady state, the serosal NaCl Ringer's was replaced with K_2SO_4 Ringer's. This caused V_t to decrease to a value of zero mV. Equal aliquots of NaCl were then added to the mucosal and serosal solutions to final concentrations of 13.3, 26.7, 40, 53.3 and 66.7 mM. Resistance and spontaneous potentials were then monitored and, since in other work with nystatin (Lewis *et al.*,

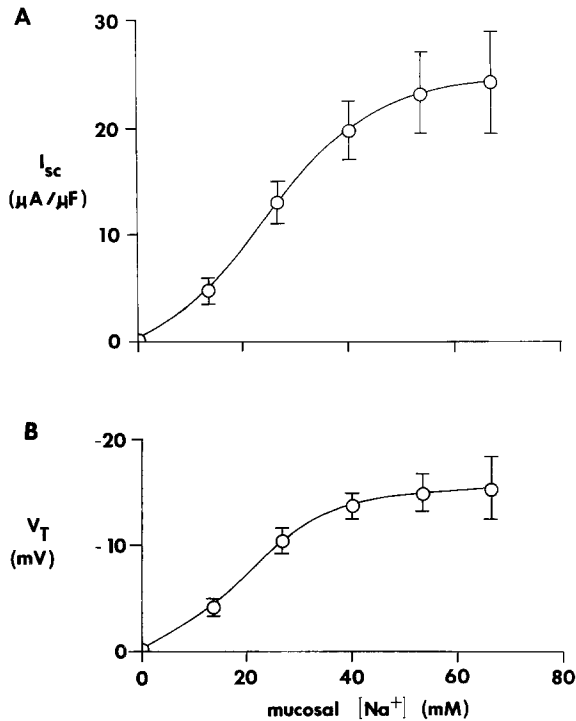


Fig. 6. Response of nystatin-treated bladders to step increases in mucosal $[Na^+]$. Short-circuit current (a) and transepithelial potential (b) are markedly increased as a function of $[Na^+]$. Solid lines were fitted by eye

1977) the basolateral $I - V$ relationship was linear, the membrane current was calculated using Ohm's Law. Figure 6a shows the current calculated for step changes in the mucosal $[Na^+]$ (serosal $[Na^+]$ had no measurable effect on V_i nor R_i). As is obvious from the figure, increasing mucosal and consequently intracellular $[Na^+]$ causes the basolateral membrane potential to become negative inside with respect to the serosal solution (Fig. 6b). To see whether this hyperpolarization and increase in current was caused by the $Na^+ - K^+$ ATPase which Lewis and Diamond (1976) previously assayed in isolated bladder membrane fragments, the tissue was first incubated for 60 min in 1×10^{-4} M ouabain (serosal solution only) and the above experiment repeated. We found that ouabain reduced the current and hyperpolarization by approximately 79 and 73 %, respectively.

The time course of the ouabain effect is shown in Figs. 7 and 8. Since serosal solution changes are performed isovolumically (time for one change ≈ 30 sec) and a supramaximal dose of ouabain used (10^{-4} M), we

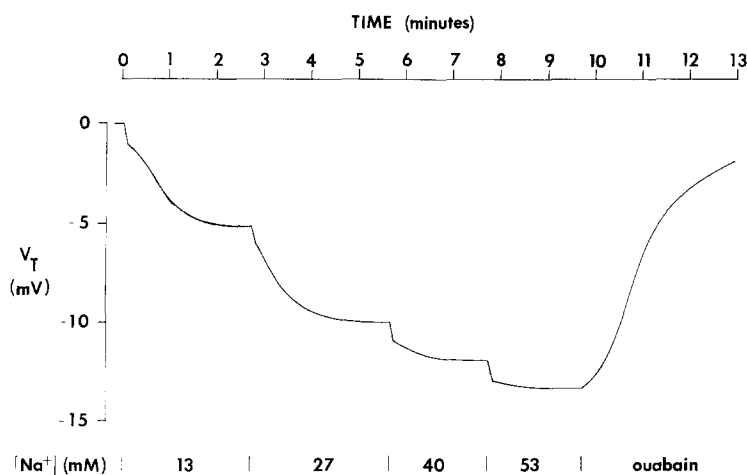


Fig. 7. Change of the basolateral potential after stepwise addition of NaCl to mucosal and serosal solutions in a nystatin-treated preparation. Ouabain (10^{-4}) was added to serosal solution and reduced the potential from 13.5 to 1.5 mV. The step change in potential after each addition of NaCl most probably represents a diffusion potential at the apical membrane. The sum of the step changes was 4 mV, yet ouabain reduced the total potential to 1.5 mV. Consequently, mucosal $[\text{Na}^+]$ and cell $[\text{Na}^+]$ were near equilibrium

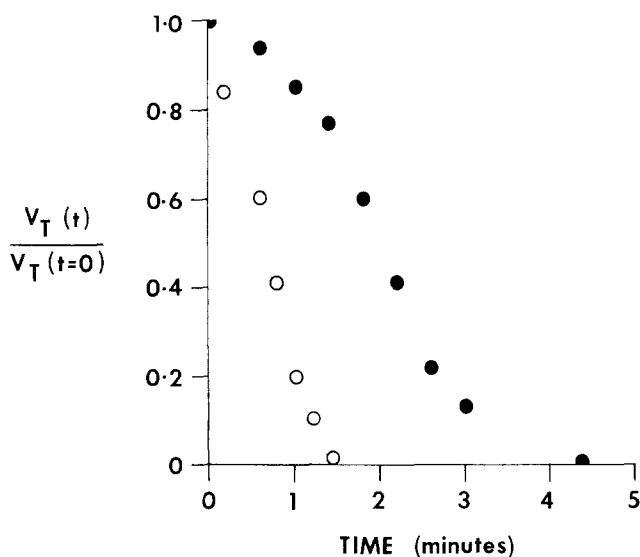


Fig. 8. Time course of ouabain inhibition of basolateral membrane hyperpolarization in two experiments. Data is normalized by dividing the measured potential $V_T(t)$ immediately before ouabain addition (10^{-4}) into the potential at time (t) after ouabain addition

cannot use the time course of the ouabain effect to estimate the thickness of the serosal unstirred layer. However, since the effect was rapid (total time of $\simeq 60\text{--}180$ sec) and the unstirred layer might be estimated at $\simeq 300\text{ }\mu\text{m}$, the rate of ouabain action must be extremely rapid, unstirred layer limited and, consequently, cannot be resolved using this technique. This rapid depolarization is in contrast to the slow depolarization shown in Fig. 5.

Discussion

In this section we discuss, in turn, intracellular ion activities in rabbit urinary bladder compared to other biological tissues, the relationship of these intracellular ion activities to the basolateral membrane potential, and a predictive electrical circuit for Na^+ transport across rabbit urinary bladder.

Comparison of Intracellular Ion Activities

The present findings have demonstrated that in the rabbit urinary bladder intracellular (K^+) is high compared to extracellular (K^+), while intracellular (Cl^-) is low compared to its extracellular activity. Similar findings have been reported for *necturus* proximal tubule (Khuri *et al.*, 1972b), *amphiuma* distal tubule (Khuri, Aguilian & Kalloghlian, 1972a), bullfrog small intestine (Lee & Armstrong, 1972), *amphiuma* small intestine (White, 1976), and toad urinary bladders (Kimura *et al.*, 1977).

Our values for intracellular (K^+) indicate that K^+ is not in electrochemical equilibrium across the basolateral membrane of rabbit bladder, similar to findings in bullfrog or *amphiuma* small intestine (Lee & Armstrong, 1972; White, 1976) and distal tubule (Khuri *et al.*, 1972a). However, K^+ is passively distributed across *necturus* proximal tubule (Khuri *et al.*, 1972b). The measured Cl^- activity ($\simeq 16\text{ mM}$) is (within experimental error) in electrochemical equilibrium across rabbit urinary bladder basolateral membrane. We made no attempt at measuring the intracellular $[\text{K}^+]$, $[\text{Na}^+]$ or $[\text{Cl}^-]$ because we felt that we could not selectively remove the first (most apical) cell layer intact to measure the ion concentrations and, consequently, could not estimate activity coefficients.

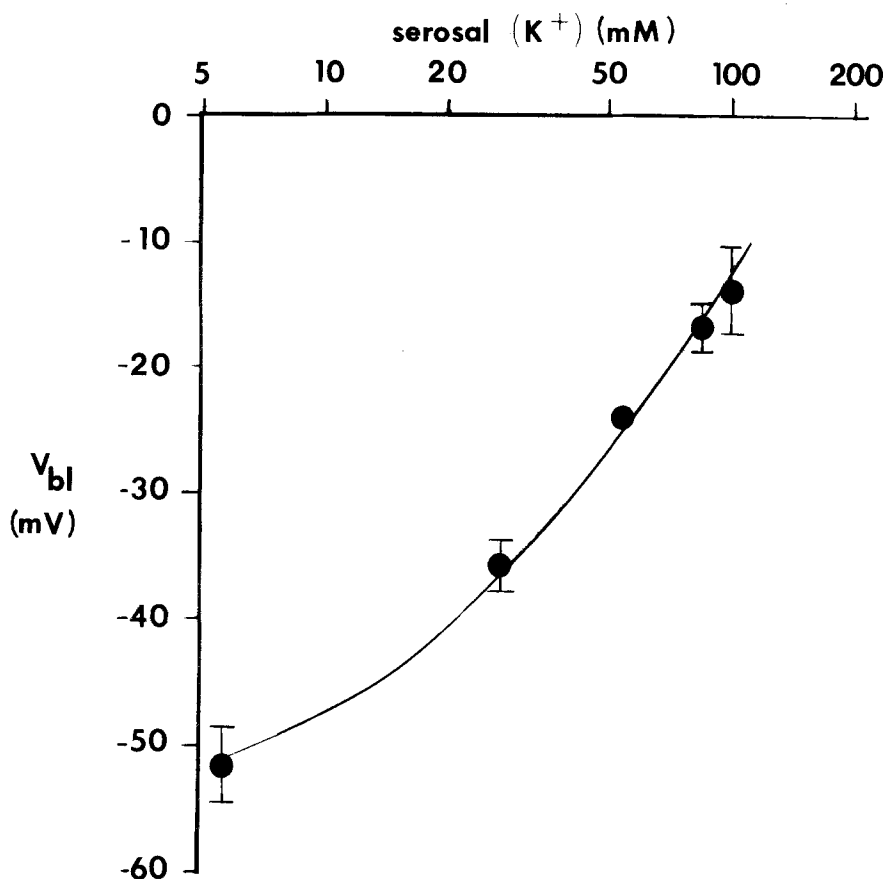


Fig. 9. An estimate of intracellular (K⁺) was obtained by curve fitting the measured spontaneous basolateral potential at different (K⁺) in serosal solution (serosal Cl⁻ constant) to the Goldman equation. P_{Na}/P_K and P_{Cl}/P_K as previously estimated, intracellular (Cl⁻) = 12 mM. The best fit value for (K⁺) was 80 mM

To check the validity of our intracellular (K⁺) measurements we have used the Goldman equation

$$V_{Bl} = \frac{RT}{ZF} \ln \cdot \frac{(K^+)_o + \frac{P_{Na}}{P_K} (Na^+)_o - \frac{P_{Cl}}{P_K} (Cl^-)_i}{(K^+)_i + \frac{P_{Na}}{P_K} (Na^+)_i + \frac{P_{Cl}}{P_K} (Cl^-)_o} \quad (5)$$

to fit our data for basolateral potential against external (K⁺) concentration at constant serosal (Cl⁻) to arrive at a value for intracellular (K⁺). We let $P_{Na}/P_K = 0.044$, $P_{Cl}/P_K = 1.17$, (Cl⁻)_i = 12 mM, (Cl⁻)_o = 92 mM,

$(\text{Na}^+)_i = 0$. Since both $(\text{Cl}^-)_o$ and $(\text{K}^+)_i$ are large numbers, setting $(\text{Na}^+)_i$ within a range of zero to 50 mM did not significantly alter our estimate of $(\text{K}^+)_i$. Our best fit intracellular K^+ activity is 80 ± 8 mM (SD) (Fig. 9), a value in good agreement with our measured value of 72 mM.

Relative Permeability of the Basolateral Membrane

The $P_{\text{Na}}/P_{\text{K}}$ of the basolateral membrane of the rabbit bladder was estimated by varying the serosal (K^+) from 1.9 to 15 mM, while maintaining a serosal constant KCl product. Above 35 mM (K^+) we found marked deviations of the membrane potential from the theoretical curve. Such deviations of the potential from predicted behavior can have a number of explanations:

1) The high external (K^+) might cause a decrease in the $P_{\text{Na}}/P_{\text{K}}$ ratio. The effect of high extracellular (K^+) on the $P_{\text{Na}}/P_{\text{K}}$ of membranes has been studied in HeLa cells (Okada, 1973) and the mucosal membrane of rat duodenum (Okada, Toshinori & Inouye, 1975). For both of these preparations $P_{\text{Na}}/P_{\text{K}}$ decreased as the extracellular (K^+) increased. In contrast, Reuss and Finn (1975) found that the $P_{\text{Na}}/P_{\text{K}}$ of the mucosal membrane of the *necturus* gallbladder increased as extracellular (K^+) increased. However, for the rabbit bladder the deviation of the basolateral potential from the predicted curve is too large to be completely accounted for by a decrease in $P_{\text{Na}}/P_{\text{K}}$.

2) Our assumption that the replacement anion (sulfate) is impermeable might be incorrect. We found a similar deviation of the incorrect basolateral membrane potential using the anion methanesulfonate, which is believed to be impermeable in other tight epithelia, but might not be.

3) Even though we used a constant KCl product, cell swelling might still occur at higher (K^+) (due to a permeable anion other than Cl^-) causing a hyperpolarization of the basolateral membrane. Finn and Reuss (1975) found that hypo-osmotic serosal solutions caused no significant change in the basolateral membrane potential of toad bladder. Preliminary results (Lewis, S.A., *unpublished observation*) on the effect of 1/2 concentration Na_2SO_4 Ringer's serosal solution on the basolateral potential showed a marked hyperpolarization of the basolateral membrane from 53 to 75 mV.

At present we have not assessed these possibilities but we feel that the reported $P_{\text{Na}}/P_{\text{K}}$ represents a reasonable value for the permeability ratio of the basolateral membrane.

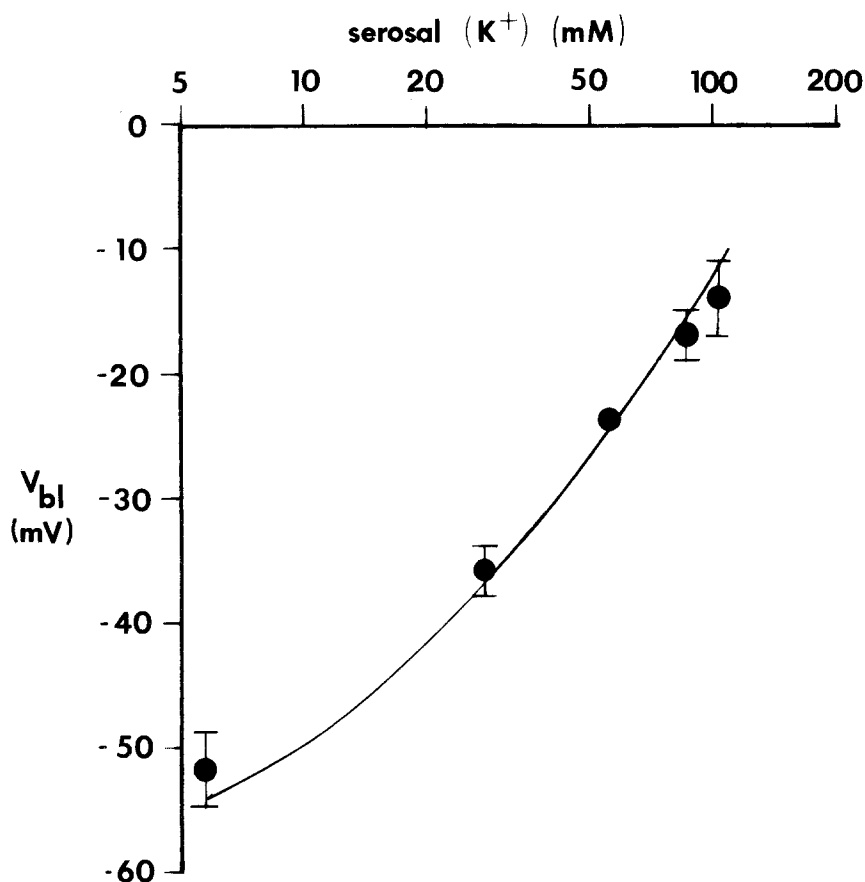


Fig. 10. Estimates of P_{Na}/P_K and P_{Cl}/P_K were obtained by performing a least squares curve fit of the measured spontaneous basolateral membrane potential at different (K^+) in serosal solution (serosal (Cl^-) constant) to the Goldman equation. Values used were intracellular $(K^+) = 72$ mM, $(Cl^-) = 12$ mM. The best fit values for P_{Na}/P_K and P_{Cl}/P_K were 0.05 and 1.0, respectively, in good agreement with previous independent estimates of 0.044 and 1.17

To verify the previous estimates of P_{Na}/P_K and P_{Cl}/P_K we fitted the Goldman equation (5) using a nonlinear curve-fitting routine for both P_{Na}/P_K and P_{Cl}/P_K to our data of basolateral potential against external (K^+) at constant serosal (Cl^-) . Intracellular $(K^+) = 72$ mM (activity), intracellular $(Cl^-) = 12$ mM, intracellular $(Na^+) = 0$ (again varying intracellular (Na^+) from 0 to 50 mM had negligible effect on the fitted values), serosal $(Cl^-) = 92$ mM and serosal K^+ and Na^+ varied but maintained a constant mass balance. The best fit P_{Na}/P_K and P_{Cl}/P_K were 0.05 and 1.0, respectively (Fig. 10), in good agreement with the independent estimates of 0.044 and 1.17.

The low $P_{\text{Na}}/P_{\text{K}}$ of the rabbit bladder basolateral membrane is consistent with the results of Canessa, Labarca and Leaf (1976) in which they found a negligible amount of Na^+ being recycled through the basolateral membrane of the toad bladder. Comparable values of $P_{\text{Na}}/P_{\text{K}}$ have also been measured for the apical membrane of rat duodenum (Okada *et al.*, 1975), and *necturus* gallbladder (Reuss & Finn, 1975).

Permeability coefficients for the basolateral membrane can be calculated from the equation (assuming ion independence and equilibrium conditions)

$$\frac{G_{bl}}{P_{\text{K}}} = \frac{z^2 F^2}{RT} \left(\bar{c}_{\text{K}} + \frac{P_{\text{Na}}}{P_{\text{K}}} \bar{c}_{\text{Na}} + \frac{P_{\text{Cl}}}{P_{\text{K}}} \bar{c}_{\text{Cl}} \right) \quad (6)$$

since

$$G_{bl} = \sum_i^n G_i,$$

and

$$G_i = P_i \frac{z^2 F^2}{RT} \bar{c}_i,$$

\bar{c}_i is the mean concentration of i^{th} ion $\bar{c}_i = \frac{c_i(\text{serosa}) - c_i(\text{cell})}{\ln \frac{c_i(\text{serosa})}{c_i(\text{cell})}}$ and R , T , z ,

F have their usual meaning. G_{bl} (mhos/cm²) is the basolateral conductance (790 $\mu\text{mhos/cm}^2$; Lewis *et al.*, 1977); $P_{\text{Na}}/P_{\text{K}}$ and $P_{\text{Cl}}/P_{\text{K}}$ as calculated (*see Results*). Calculated values are $P_{\text{K}} = 2.27 \times 10^{-6}$ cm/sec, $P_{\text{Cl}} = 2.65 \times 10^{-6}$ cm/sec and $P_{\text{Na}} = 0.1 \times 10^{-6}$ cm/sec, $G_{\text{K}} = 277$ mhos/cm², $G_{\text{Cl}} = 497 \times 10^{-6}$ mhos/cm² and $G_{\text{Na}} = 17.1 \times 10^{-6}$ mhos/cm².

Basolateral Membrane Potential: Passive and Active Components

1. Diffusion potential. In contrast to toad bladder, the basolateral membrane potential for the rabbit urinary bladder, at steady state, is indeed a K^+ diffusion potential attenuated by a finite Na^+ permeability ($P_{\text{Na}}/P_{\text{K}} = 0.044$) whose gradient is oriented in a direction opposite to the K^+ gradient. Cl^- seems to be in electrochemical equilibrium across the basolateral membrane and consequently does not influence the basolateral membrane potential (for steady-state conditions). However, an alteration of serosal Cl^- activity will cause transient changes in the basolateral membrane potential.

2. *Electrogenic potential.* One of the most interesting results we found was the existence of an electrogenic pump which is rapidly inhibited with ouabain (we feel that the time course of ouabain action is unstirred layer limited in our experiments). An electrogenic pump with a comparable maximal voltage (14 mV) has been found by Rose, Nahrwold and Koch (1977) in rabbit ileum. We must stress that for the normal transport rate of the rabbit urinary bladder (unlike the ileum) there is no evidence that the electrogenic pump contributes to the basolateral membrane potential. This suggests that if the transport process in the normal bladder has stoichiometry similar to that of a nystatin-treated bladder then the intracellular $[\text{Na}^+]$ is probably less than 13 mM, since 13 mM Na^+ caused a 5-mV hyperpolarization of the basolateral membrane in a treated bladder (Fig. 6b). The transport process is a saturable process where ≈ 66 mM intracellular $[\text{Na}^+]$ will represent the maximum value for saturation (Figs. 6a–b and 7, assuming equilibration between mucosal and intracellular Na^+).

In addition, the pump current as a function of $[\text{Na}^+]$ is not adequately described by Michaelis-Menten kinetics, as is obvious from the sigmoidal shape. Some possible explanations for this are:

1) The intracellular $[\text{Na}^+]$ is less than the mucosal $[\text{Na}^+]$ after nystatin addition. We can speculate that the ratio of intracellular to mucosal $[\text{Na}^+]$ will be a low value at low mucosal $[\text{Na}^+]$. This ratio will approach unity as mucosal $[\text{Na}^+]$ is increased. To quantitate such a possibility it would be necessary to measure the intracellular (Na^+) as a function of mucosal (Na^+) and I_{sc} .

2) A kinetic model with fixed coupling ratio (3:2 for Na^+/K^+) derived by Lindenmayer, Schwartz and Thompson (1974) predicts a sigmoidal relationship between $[\text{Na}^+]$ at ATP hydrolysis at constant $[\text{K}^+]$. Their model fits our data reasonably well below a $[\text{Na}^+]$ of 27 mM; above this $[\text{Na}^+]$, there is a consistent deviation of the data from the theoretical curve which could be accounted for by a variable (increasing) coupling ratio.

3) The nonphysiological conditions under which this experiment was conducted might alter the kinetics of the $\text{Na}^+ - \text{K}^+$ ATPase. Lindenmayer *et al.* (1974) found, for purified red cell $\text{Na}^+ - \text{K}^+$ ATPase, that an increase in $[\text{K}^+]$ reduces the activation of the ATPase at any fixed $[\text{Na}^+]$. Thus, our I_{sc} as a function of mucosal $[\text{Na}^+]$ might represent a minimum value.

The basolateral potential in a normal transporting rabbit bladder is primarily a diffusion potential with K^+ and Cl^- the most permeable ions

with only a small (<2 mV) electrogenic contribution. As the Na^+ transport rate increases, the electrogenic component will become more evident. The magnitude of the electrogenic component on the measured basolateral potential will be dependent on the coupling ratio as well as the junctional resistance.

Addition to a Model

The present results indicate that the classic Koefoed-Johnsen and Ussing model for Na^+ transport across a tight epithelium is in need of expansion. A brief description of a more complete model is as follows: Na^+ entry across the apical membrane occurs passively via an amiloride-sensitive, aldosterone-stimulated Na^+ specific conductance pathway. The driving force for Na^+ entry is assumed to be the sum of the electrical and chemical (Na^+) gradients across this membrane. Na^+ extrusion across the basolateral membrane must be mediated by an active transport system, presumably the $\text{Na}^+ - \text{K}^+$ activated, ouabain-inhibited ATPase found in bladder membrane fragments. Intracellular (Na^+) (or some other entity; e.g., Ca^{2+} , H^+ , K^+ , Cl^-) regulates the apical Na^+ conductance; i.e., there is a negative feedback system whereby an increase in intracellular (Na^+) caused by an increase in Na^+ entry from the mucosal solution or a decrease in Na^+ extrusion across the basolateral membrane (e.g., ouabain inhibition of the basolateral pump) causes a decrease in Na^+ conductance and thus entry across the apical membrane (see Lewis *et al.*, 1976; and Lewis, 1977*a-b*, for more detail).

To this model we add the following elements:

- 1) Intracellular K^+ and Cl^- activities are 72 and 16 mM, respectively.
- 2) $P_{\text{Na}}/P_{\text{K}}$ and $P_{\text{Cl}}/P_{\text{K}}$ for basolateral membrane are 0.044 and 1.17, respectively ($P_{\text{K}} = 2.27 \times 10^{-6}$, $P_{\text{Na}} = 0.1 \times 10^{-6}$, $P_{\text{Cl}} = 2.65 \times 10^{-6}$ cm/sec).
- 3) The source of the basolateral membrane potential (≈ 52 mV cell interior negative with respect to the serosal solution) is a K^+ and Cl^- diffusion potential attenuated by a finite Na^+ permeability.
- 4) Cl^- is passively distributed across the basolateral membrane.
- 5) There is ouabain-sensitive electrogenic transport system located at the basolateral membrane. The coupling ratio as a function of intracellular (Na^+) is not presently known.
- 6) We estimate that if the stoichiometry of the Na^+ transport process is the same under normal conditions as when the apical membrane is treated with nystatin then intracellular $[\text{Na}^+] < 13$ mM.

An Electrical Equivalent Circuit for Rabbit Bladder

From collected experimental observations (such as those illustrated in this paper), we have derived an electrical equivalent circuit which we feel is a reasonable approximation of the electrical properties of the rabbit urinary bladder. Figure 11 illustrates the equivalent circuit and the equations that describe three parameters of interest, transepithelial potential, basolateral potential, and short-circuit current.

1. $G_T - I_{sc}$. Does this equivalent circuit predict the $I_{sc} - G_T$ relationship for rabbit urinary bladder? Many of the individual circuit elements in the equivalent circuit have been independently measured (*see Results and Discussion*, this paper; Lewis & Diamond, 1976; Lewis *et al.*, 1976; Lewis, 1977a-b; Lewis *et al.*, 1978) (Table 3). We set R_a^K (apical K^+

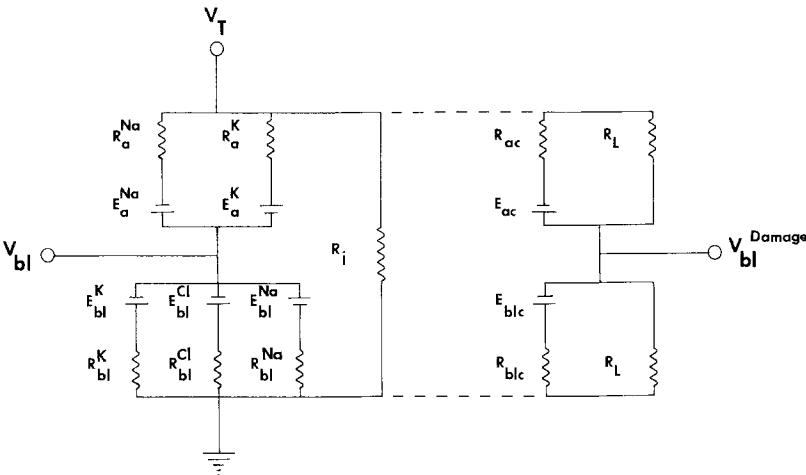


Fig. 11. A representative equivalent circuit for Na^+ transport across rabbit urinary bladder. *See text* for description of parameters

Table 3.

Apical membrane			Basolateral membrane								R_T	V_T	V_{bl}
R_a^{Na}	E_a^{Na}	R_a^K	E_a^K	R_{bl}^K	E_{bl}^K	R_{bl}^{Na}	E_{bl}^{Na}	R_{bl}^{Cl}	E_{bl}^{Cl}	R_j			
1000,000	70	100,000	70	3600	70	58000	70	2000	52	100,000	33900	-36.8	-55
50,000											25500	-58.7	-54
20,000											15200	-86.8	-54
10,000											9400	-102	-54
5,000											5670	-112	-54
2,000											3120	-120	-54

Values for the equivalent circuit as determined in this paper, and from Lewis *et al.* (1977)

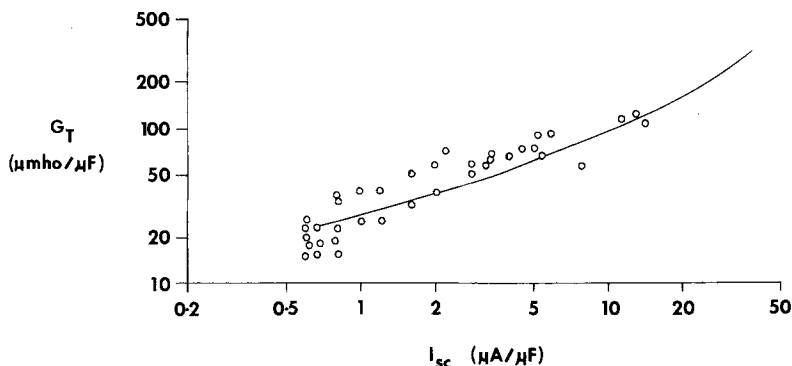


Fig. 12. Relation between transepithelial conductance and I_{sc} (from Lewis & Diamond, 1976). The line was calculated from the equivalent circuit and parameters listed in Appendix I and Table 3

resistance) at 1×10^5 ohm cm^2 , and $E_a^K = E_{bl}^K = E_a^{\text{Na}} = 70$ mV. Using Eqs. (A1) and (A2) we compute V_T , R_T and I_{sc} for R_a^{Na} of 1×10^5 to 2×10^3 ohm cm^2 . The calculated $G_T(1/R_T)$ is plotted against the calculated I_{sc} and compared to the data of Lewis and Diamond (1976) (their Fig. 16). This plot is illustrated in Fig. 12 and the predicted curve is in reasonable agreement with the experimental data.

The inverse slope of a linear plot of G_T vs. I_{sc} will, according to Yonath and Civan (1971), yield the driving force (E_{Na}) of the sodium pump (see Yonath & Civan, 1971, for assumption). The inverse slope (E_{Na}) can be expressed in terms of our equivalent circuit (Fig. 11) as:

$$E_{\text{Na}} = E_a^{\text{Na}} + E_{bl} + \frac{R_{bl}}{R_a^K} (E_a^{\text{Na}} + E_a^K) \quad (7)$$

if $R_{bl}/R_a^K \ll 1$, then $E_{\text{Na}} = E_a^{\text{Na}} + E_{bl}$; this equation is the same as the equation derived by Schultz *et al.* (1977).

Our predicted curve has an inverse slope of 127 mV. A linear regression analysis of the data points in Fig. 12 yields an inverse slope of 116 mV. These values are in close agreement with that estimated for toad urinary bladder of 105–158 mV (Yonath & Civan, 1971; Saito, Lief & Essig, 1974; Chen & Walser, 1975) and rabbit descending colon of 117 mV (Schultz *et al.*, 1977). The difference in the predicted and best fit inverse slopes for rabbit bladder is probably caused by our overestimate of E_a^{Na} .

Our predicted curve is based on the assumption that all changes in I_{sc} are caused solely by changes in G_a^{Na} . In essence this assumption is the

same as that made by Yonath and Civan (1971) for the calculation of E_{Na} . That this assumption is not strictly valid might account for the deviations of the predicted curve from the experimental points (see Fig. 12). A more quantitative equivalent circuit must consider the effects of intracellular Na^+ activity on apical membrane conductance (G_a^{Na}) and potential (E_a^{Na}) (negative feedback hypothesis, MacRobbie & Ussing, 1961; Ussing, Erlj & Lassen, 1974; Lewis *et al.*, 1976) as well as on the basolateral membrane potential (E_{bl}) and possibly conductance (G_{bl}) (electrogenic pump).

We are presently unable to construct such an equivalent circuit due to the lack of quantitative data on the relationship between intracellular Na^+ activity and membrane conductances and potentials. However, we feel that a more interactive model would produce a quantitative difference from the analysis presented here only at high transport rates ($> 20 \mu\text{A}/\text{cm}^2$).

2. Unified Model? All of our data suggest that with some modification the Koefoed-Johnsen and Ussing theory is adequate to explain Na^+ transport in the rabbit bladder. This is in contrast to the viewpoint offered in a recent review article (Finn, 1976) where evidence was offered that the basolateral membrane and apical membrane potentials of toad urinary bladder are not K^+ and Na^+ diffusion potentials, respectively. We address ourselves to the question of whether rabbit urinary bladder and toad urinary bladder perform the function of Na^+ transport by two different methods, even though from black-box analysis both preparations behave in a similar manner (see Lewis *et al.*, 1976). Thus amiloride, reduced mucosal $[\text{Na}^+]$, and ouabain inhibit Na^+ transport and increase transepithelial resistance, while aldosterone and elevated mucosal $[\text{Na}^+]$ increases Na^+ transport and decreases transepithelial resistance.

Finn (1976) found that the change in the transepithelial potential (ΔV_T) caused by a step increase in the serosal $[\text{K}^+]$ for a range of steady-state transepithelial potentials (transepithelial potential (V_T) was altered using amiloride, ouabain or cold), produced a linear relationship between V_T and ΔV_T . The Koefoed-Johnsen and Ussing model should, according to the review, yield a relationship in which ΔV_T is independent of V_T . The equivalent circuit used to draw this conclusion was a series combination of 2 batteries and 2 resistors, a K^+ battery and its corresponding resistor (basolateral membrane) and a Na^+ battery and its corresponding resistor (apical membrane). This circuit has left out one of the most important components of any tight or leaky epithelium, a parallel resistance, that

will attenuate the sum of the two membrane batteries. This resistance is due either to the resistance of the junctional complexes or to shunting caused by edge damage. Thus, the absolute resistance of the junction (R_j) in conjunction with the apical and basolateral membrane resistances (R_a and R_{bl}) and batteries (E_a and E_{bl}) forms an equation which will determine the transepithelial potential (V_T) [Eq. (A1), Appendix 1]. By simply making R_j finite, this linear relationship is predicted by a revised version of the Koefoed-Johnsen and Ussing model proposed by Lewis *et al.* (1976), and Lewis (1977a). In this modified version amiloride directly and ouabain indirectly (through a negative feedback system) increases R_a (and either increases or decreases E_a), while leaving E_{bl} and R_{bl} unaltered.

From Eq. (A1) it is obvious that when we apply amiloride, R_a will increase causing a decrease in V_T . The ΔV_T caused by the step change in serosal (K^+) will be less than the ΔV_T before amiloride addition, yielding a near linear relationship between V_T and ΔV_T .

Thus, the above evidence offered by Finn (1976) to disclaim the Koefoed-Johnson and Ussing model in toad bladder is actually consistent with the model if the appropriate equivalent circuit of the epithelium is used.

We feel that there is still no convincing evidence that the major source of the basolateral potential of urinary bladder is anything other than a diffusion potential with K^+ and Cl^- being the most permeable ions and that the apical membrane potential at high transport rates is primarily a sodium diffusion potential. On the other hand, the long standing Koefoed-Johnson and Ussing model is in need of elaboration, a process to which this paper has addressed itself.

Appendix 1

We consider and derive an equivalent electrical circuit which is a reasonable approximation for the description of the electrical phenomena of Na^+ transport across the rabbit urinary bladder. (Similar circuits have been derived by Rose & Schultz, 1971.) We also consider the effect that a microelectrode impalement shunt, in either or both apical and basolateral membranes, will have on the measured apical and basolateral membrane potentials at different transport rates (I_{sc}).

Figure 11 (left) is a schematic representation of the equivalent circuit and illustrates the batteries and resistors that compose the apical mem-

branes (E_a^i and R_a^i where i is the ion species) and basolateral membrane (E_{bl}^i and R_{bl}^i). R_j is the tight junction resistance.

We can describe the transepithelial potential (V_T) as:

$$V_T = -\frac{E_a + E_{bl}}{R_a + R_{bl}} \cdot R_T \quad \text{or} \quad = -\frac{(E_a + E_{bl}) R_j}{R_a + R_{bl} + R_j} \quad (\text{A1})$$

where

$$\begin{aligned} E_a &= \left(\frac{E_a^{\text{Na}}}{R_a^{\text{Na}}} - \frac{E_a^{\text{K}}}{R_a^{\text{K}}} \right) \cdot R_a \quad \text{where} \quad R_a = \frac{R_a^{\text{Na}} R_a^{\text{K}}}{R_a^{\text{Na}} + R_a^{\text{K}}} \\ E_{bl} &= \left(\frac{E_{bl}^{\text{K}}}{R_{bl}^{\text{K}}} - \frac{E_{bl}^{\text{Na}}}{R_{bl}^{\text{Na}}} + \frac{E_{bl}^{\text{Cl}}}{R_{bl}^{\text{Cl}}} \right) \cdot R_{bl} = \frac{R_{bl}^{\text{K}} R_{bl}^{\text{Na}} R_{bl}^{\text{Cl}}}{R_{bl}^{\text{K}} R_{bl}^{\text{Na}} + R_{bl}^{\text{Na}} R_{bl}^{\text{Cl}} + R_{bl}^{\text{K}} R_{bl}^{\text{Cl}}} \\ R_T &= \frac{(R_a + R_{bl}) R_j}{R_a + R_{bl} + R_j} \\ I_{sc} &= \frac{V_T}{R_T} \end{aligned} \quad (\text{A2})$$

and the basolateral potential as:

$$\begin{aligned} V_{bl} &= -\left(\frac{E_{bl}}{R_{bl}} - \frac{E_a}{R_a + R_j} \right) \cdot \frac{(R_a + R_j) R_{bl}}{R_a + R_{bl} + R_j} \\ &= \frac{-E_{bl}(R_a + R_j) + E_a R_{bl}}{R_a + R_{bl} + R_j}. \end{aligned}$$

The apical membrane potential is then the difference between the trans-epithelial and basolateral potentials.

$$V_a = V_T - V_{bl}.$$

Equivalent circuit (Fig. 11, right connected to circuit *A* via the broken line) represents a single cell where R_{ac} is equivalent to R_a times the ratio of the epithelial surface area to the surface area of a single cell. Thus

$$R_{ac} = R_a \cdot \frac{\text{epithelial area}}{\text{single cell area}} \quad (\text{ratio} = 250,000).$$

R_L is the shunt resistance introduced into the apical and/or basolateral membrane of a single cell during a microelectrode impalement.

The basolateral potential of this damaged cell is

$$V_{bl}^{\text{Damage}} = -\left(\frac{V_T - E_{aD}}{R_{aD} + R_T} + \frac{E_{blD}}{R_{blD}} \right) \cdot \frac{(R_{aD} + R_T) R_{blD}}{R_{aD} + R_T + R_{blD}} \quad (\text{A3})$$

where

$$E_{aD} = \frac{E_a R_L}{R_{ac} + R_L} \quad R_{bID} = \frac{R_{blc} R_L}{R_{lc} + R_L}.$$

This is a simplified equation where we have assumed that a single damaged cell will not significantly alter V_T by a shunting effect; i.e., we assume R_{ac} , R_{blc} and $R_L \gg R_j$.

Using Eq. (A3) and the determined values for the circuit elements (Table 3) we investigate the effect of microelectrode impalement damage on the measured apical and basolateral membrane potentials (V_a and V_{bl} , respectively) at different transport rates (I_{sc}). We mimic the effect of amiloride (reported to decrease the Na^+ selective conductance pathway in the apical membrane, Lewis *et al.*, 1976) on decreasing the I_{sc} and increasing R_T by increasing the value of R_a^{Na} , while leaving all other parameters unaltered.

We investigate four cases:

Case I. No impalement damage: Figure 13a, a plot of V_a and V_{bl} against I_{sc} illustrates that as I_{sc} decreases (after amiloride application), V_a depolarizes while V_{bl} hyperpolarizes a small amount (≈ 1 mV).

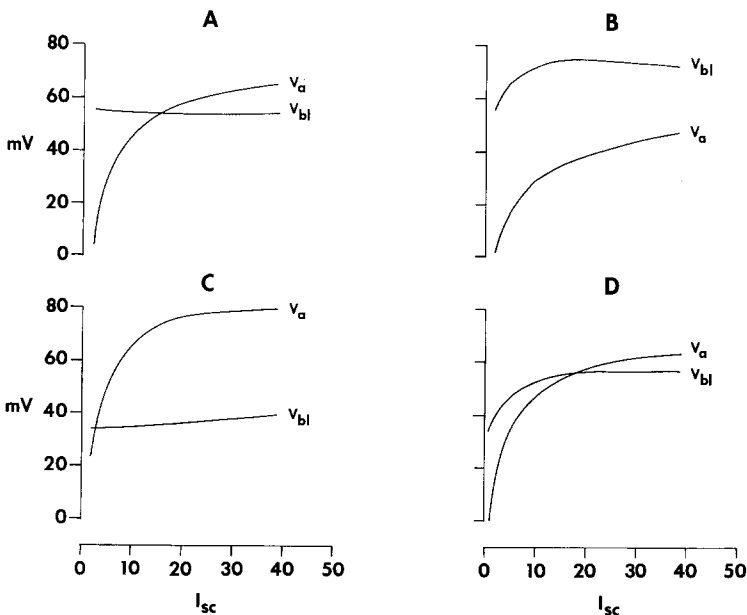


Fig. 13. The effect of microelectrode impalement damage to the apical (b), basolateral (c) or both membranes (d) on V_a (apical spontaneous potential) and V_{bl} basolateral spontaneous potential) as a function of I_{sc} . Theoretical lines were calculated using Eq. (A3) (Appendix I). (a): Control—no damage

Case II. Impalement damage in apical membrane only. Figure 13*b*. V_a depolarizes as I_{sc} decreases, V_{bl} transiently hyperpolarizes and then depolarizes.

Case III. Impalement damage in basolateral membrane only. Figure 13*c*. Both apical and basolateral membranes depolarize simultaneously.

Case IV. Impalement damage in both membranes. Figure 13*d*. V_a depolarizes as I_{sc} decreases, V_{bl} remains constant (within 1 mV) and then starts to depolarize when I_{sc} is significantly reduced.

Since amiloride action is a time-dependent phenomena, we can see that impalement damage of either the apical or apical and basolateral membranes could cause a time to occur between the depolarization of the apical and basolateral membrane potentials. The magnitude of depolarization of V_{bl} and V_a is dependent on the amount of damage introduced into the two membranes. The time delay will depend not only on the amount of damage, but also the initial I_{sc} . Large amounts of damage or a low initial I_{sc} will yield a short delay; conversely, less damage and a large I_{sc} will result in a longer delay.

In the above analysis we have ignored the possibility of an electrogenic pump and the effect that impalement damage will have on intracellular ion composition and thus on the parameters E_{bl}^K , E_{bl}^{Na} and E_{bl}^{Cl} . Equilibration between mucosal and intracellular solutions will reduce the magnitude of these parameters, resulting in a reduction in the time delay between the two membrane parameters.

The above analysis might also explain the results of Reuss and Finn (1975). Reuss and Finn (1975) found that mucosally applied amiloride caused both apical and basolateral membrane potentials to depolarize with a 10–20 msec delay between the initiation of the apical and the basolateral membrane depolarization. This result for the toad urinary bladder (*Bufo marinus*) would seem inconsistent with the Koefoed-Johnsen and Ussing model and also the data reported by Lewis *et al.* (1976), Lewis (1977*a*) and Lewis *et al.* (1977) for rabbit urinary bladder (our equivalent circuit). In addition, Wills, Lewis and Eaton (*in preparation*) and Schultz *et al.* (1977) have demonstrated for rabbit descending colon that amiloride causes no change in the basolateral potential that cannot be accounted for by either finite junctional resistances or measured changes in the apical membrane resistances. Recently Sudou and Hoshi (1977) found that mucosal amiloride caused only small changes in basolateral potential of toad urinary bladder (*Bufo vulgaris*) when compared to the change reported by Reuss and Finn (1975). Lindemann

(1975) and Sudou and Hoshi (1977) have suggested that the results of Reuss and Finn (1975) were caused by impalement damage artifacts. However, Finn (1976) states that such a damage artifact could not account for the delay of 10 to 20 msec between the initiation of apical membrane depolarization and the basolateral membrane depolarization. If indeed our analysis is correct, we find that impalement damage can cause an apparent delay between membrane potential changes.

This work was supported by grants from the U.S. Public Health Service AM-20068 and AM-00432 to Dr. Eaton and AM-20851 to Dr. Lewis.

References

- Canessa, M., Labarca, P., Leaf, A. 1976. Metabolic evidence that serosal sodium does not recycle through the active transepithelial transport pathway of toad bladder. *J. Membrane Biol.* **30**:65
- Chen, J.S., Walser, M. 1975. Sodium fluxes through the active transport pathway in toad bladder. *J. Membrane Biol.* **21**:87
- Eaton, D.C., Russell, J.M., Brown, A.M. 1975. Ionic permeabilities of an *Aplysia* giant neuron. *J. Membrane Biol.* **21**:353
- Finn, A.L. 1976. Changing concepts of transepithelial sodium transport. *Physiol. Rev.* **56**:453
- Finn, A.L., Reuss, L. 1975. Effects of changes in the composition of the toad urinary bladder epithelium. *J. Physiol. (London)* **250**:541
- Fuch, W., Hviid Larsen, E., Lindemann, B. 1977. Current-voltage curve of sodium channels and concentration dependence of sodium permeability in frog skin. *J. Physiol. (London)* **267**:137
- Helman, S.I., Fisher, R.S. 1977. Microelectrode studies of the active Na transport pathway of frog skin. *J. Gen. Physiol.* **69**:571
- Khuri, R.N., Agulian, S.K., Kalloghlian, A. 1972a. Intracellular potassium in cells of the distal tubule. *Pfluegers Arch.* **338**:73
- Khuri, R., Hajjar, J.J., Agulian, S., Bogharian, K., Kalloghlian, A., Bizri, H. 1972b. Intracellular potassium in cells of the proximal tubule of *Necturus maculosus*. *Pfluegers Arch.* **338**:73
- Kimura, G., Urakabe, S., Yuasa, S., Miki, S., Takamitsu, Y., Orita, Y., Abe, H. 1977. Potassium activity and plasma membrane potentials in epithelial cells of toad bladder. *Am. J. Physiol.* **232**:F196
- Koefoed-Johnsen, V., Ussing, H.H. 1958. The nature of the frog skin potential. *Acta Physiol. Scand.* **43**:298
- Lee, C.O., Armstrong, W.McD. 1972. Activities of sodium and potassium ions in epithelial cells of small intestine. *Science* **175**:1261
- Lewis, S.A. 1977a. A reinvestigation of the function of the mammalian urinary bladder. *Am. J. Physiol.* **232**:F187
- Lewis, S.A. 1977b. Model of sodium transport in tight epithelia. Joshua Macy, Jr., Foundation Symposia on Renal Function (*in press*).
- Lewis, S.A., Diamond, J.A. 1975. Active sodium transport by mammalian urinary bladder. *Nature (London)* **253**:747
- Lewis, S.A., Diamond, J.M. 1976. Na⁺ transport by rabbit urinary bladder, a tight epithelium. *J. Membrane Biol.* **28**:1

- Lewis, S.A., Eaton, D.C., Clausen, C., Diamond, J.M. 1977. Nystatin as a probe for investigating the electrical properties of a tight epithelium. *J. Gen. Physiol.* **70**:427
- Lewis, S.A., Eaton, D.C., Diamond, J.M. 1976. The mechanism of Na^+ transport by rabbit urinary bladder. *J. Membrane Biol.* **28**:41
- Lindemann, B. 1975. Impalement artifacts in microelectrode recordings of epithelial membrane potentials. *Biophys. J.* **15**:1164
- Lindenmayer, G.E., Schwartz, A., Thompson, H.K., Jr. 1974. A kinetic description for sodium and potassium effects on $(\text{Na}^+ - \text{K}^+ - \text{adenosine triphosphatase})$. A model for a two-nonequivalent site potassium activation and an analysis of multivalent site models for sodium activation. *J. Physiol. (London)* **236**:1
- MacRobbie, E.A.C., Ussing, H.H. 1961. Osmotic behavior of the epithelial cells of frog skin. *Acta Physiol. Scand.* **36**:17
- Okada, Y., Ogawa, M., Aoki, N., Izutsu, K. 1973. The effect of K^+ on the membrane potential in Hela cells. *Biochim. Biophys. Acta* **291**:116
- Okada, Y., Toshinori, S., Inouye, A. 1975. Effects of potassium ions and sodium ions on membrane potential of epithelial cells in rat duodenum. *Biochim. Biophys. Acta* **413**:104
- Reuss, L., Finn, A.L. 1975. Electrical properties of the cellular transepithelial pathway in *Necturus* gall bladder: II. Ionic permeability of the apical cell membrane. *J. Membrane Biol.* **25**:141
- Reuss, L., Finn, A.L. 1976. Dependence of serosal membrane potential on mucosal membrane potential in toad urinary bladder. *Biophys. J.* **15**:71
- Rose, R.C., Narwold, D.L. and Koch, M.J. 1977. Electrical potential profile in rabbit ileum: Role of rheogenic Na^+ transport. *Am. J. Physiol.* **232**:E5
- Rose, R.C., Schultz, S.G. 1971. Studies on the electrical potential profile across rabbit ileum. *J. Gen. Physiol.* **57**:639
- Russell, J.M., Eaton, D.C., Brodwick, M.S. 1977. Effects of nystatin on membrane conductance and internal ion activities in *Aplysia* neurons. *J. Membrane Biol.* **37**:137
- Saito, T., Lief, P.D., Essig, A. 1974. Conductance of active and passive pathways in the toad bladder. *Am. J. Physiol.* **226**:1265
- Schultz, S.G., Frizzell, R.A., Nellans, H.N. 1977. Active sodium transport and the electrophysiology of rabbit colon. *J. Membrane Biol.* **33**:351
- Sudou, K., Hoshi, T. 1977. Mode of action of amiloride in toad urinary bladder. *J. Membrane Biol.* **32**:115
- Turnheim, K., Frizzell, R.A., Schultz, S.G. 1977. Effect of anions on amiloride-sensitive, active sodium transport across rabbit colon, *in vitro*. *J. Membrane Biol.* **37**:63
- Ussing, H.H., Erlj, D., Lassen, U. 1974. Transport pathways in biological membranes. *Annu. Rev. Physiol.* **36**:17
- Walker, J.L. 1971. Ion specific liquid ion exchanger microelectrodes. *Anal. Chem.* **43**:89a
- White, J.F. 1976. Intracellular potassium activities in *Amphiuma* small intestine. *Am. J. Physiol.* **321**:1214
- Yonath, J., Civan, M.M. 1971. Determination of the driving force of the Na^+ pump in toad bladder by means of vasopressin. *J. Membrane Biol.* **5**:366